# Lateral spreading and flooding along the İskenderun coast in the 2023 Kahramanmaraş earthquake sequence

Patrick Bassal i), Diane M. Moug ii), Jonathan D. Bray iii), Sena B. Kendır iv), K. Onder Cetin v), and Arda Şahin vi)

i) Assistant Professor, Department of Civil, Environmental, and Geodetic Engineering, The Ohio State University, OH, USA
 ii) Assistant Professor, Department of Civil and Environmental Engineering, Portland State University, OR, USA
 iii) Distinguished Professor, Civil and Environmental Engineering Department, University of California, Berkeley, CA, USA
 iv) Engineer, Zemin Etud ve Tasarim A.S., Istanbul, Türkiye
 v) Professor, Civil Engineering Department, Middle East Technical University, Ankara, Türkiye
 vi) Ph.D. Student, Civil and Environmental Engineering Department, University of California, Los Angeles, CA, USA

### **ABSTRACT**

The 2023 Kahramanmaraş earthquake sequence produced extensive liquefaction-induced ground deformations along the infilled shoreline of the port city of İskenderun, Türkiye. Observed liquefaction effects included ground settlement, seaward lateral spreading, and failures along a rubble mound seawall lining the coast. These effects, among other factors, likely contributed to ongoing flooding in İskenderun during moderate storm and high tide events following the earthquakes. The Geotechnical Extreme Events Reconnaissance (GEER) team collected detailed observations and measurements of selected sites affected by liquefaction. This paper presents lateral spreading, ground settlement, and flooding observations in İskenderun, which suggest widespread movements of the coastline relative to the current sea level. The Doğan restaurant case history is described in detail, where earthquake ground deformations and subsequent flooding damaged a dining patio, seawall, and nearby park facilities. Insights from these observations suggest a need to better understand multi-hazard liquefaction and flood consequences to enhance the resilience of coastal cities.

Keywords: Earthquake, flooding, lateral spreading, liquefaction, multi-hazard performance

## 1 INTRODUCTION

The M<sub>w</sub> 7.8 mainshock of the Kahramanmaraş earthquake sequence on February 6, 2023 caused severe damage to the Mediterranean port city of İskenderun, Hatay Province, Türkiye. İskenderun is located about 19 km to the west of the East Anatolian fault rupture (e.g., Reitman et al. 2023). Nearby ground motion stations #TK3116 (~5 km south of the İskenderun urban area) and #TK3115 (~4 km northwest of the urban area), recorded peak ground accelerations (PGAs) of 0.176 g and 0.293 g, respectively.

Several post-earthquake reconnaissance teams, including the Middle East Technical University (METU), Geotechnical Extreme Events Reconnaissance (GEER) Association, and Earthquake Engineering Research Institute (EERI) teams, were deployed to investigate damage following the Kahramanmaraş earthquake sequence. Observed liquefaction effects included widespread sediment ejecta, ground and building settlement, seaward lateral spreading, and damage to shoreline protection structures. Additionally, coastal flooding during ordinary storm and high tide events has inundated large portions of the city at an unusually frequent rate since the earthquakes occurred.

This paper presents key observations of liquefaction-induced lateral spreading and flooding in Iskenderun documented by the Turkey-US GEER team between March 28 and April 1, 2023. The Doğan restaurant case history is described, where lateral spreading and subsequent flooding damaged a dining patio, seawall, and nearby park facilities. Implications for future work intended to clarify the contributing factors for the postearthquake increase of flood hazard in İskenderun are discussed.

## 2 REGIONAL GEOLOGY AND URBAN DEVELOPMENT OF ISKENDERUN

İskenderun is located within a low-lying alluvial floodplain east of the Amanos mountains, along the İskenderun bay of the Mediterranean sea. The region is primarily composed of quaternary-age alluvium and artificial fill, with higher rates of sand and fine-grained silts and clays observed in boreholes within 1 km of the shoreline, as opposed to those further inland. The groundwater depth within the urban area is typically within 1-3 m of the ground surface (Ulu et al. 2002, Orukoğlu and İşhani 2010).

A shallow water table and an abundance of marshes

slowed the development of İskenderun (formerly known as Alexendretta) under Ottoman rule in the 19<sup>th</sup> century. The İbrahim Paşa channel system built in the 1830's was largely ineffective in draining the marshes and swamps as it was poorly maintained and gradually filled up with sediment deposits. A historic 1916 map (Fig. 1) obtained from the National Library of Turkey by Nalça (2018) depicts the early swamps and marshes, channels and built areas, and shoreline. Under the French Mandate period in the 1920's, successful interventions included filling the land, planting trees to absorb water, and building more robust concrete drainage channels (e.g., Nalça 2018).

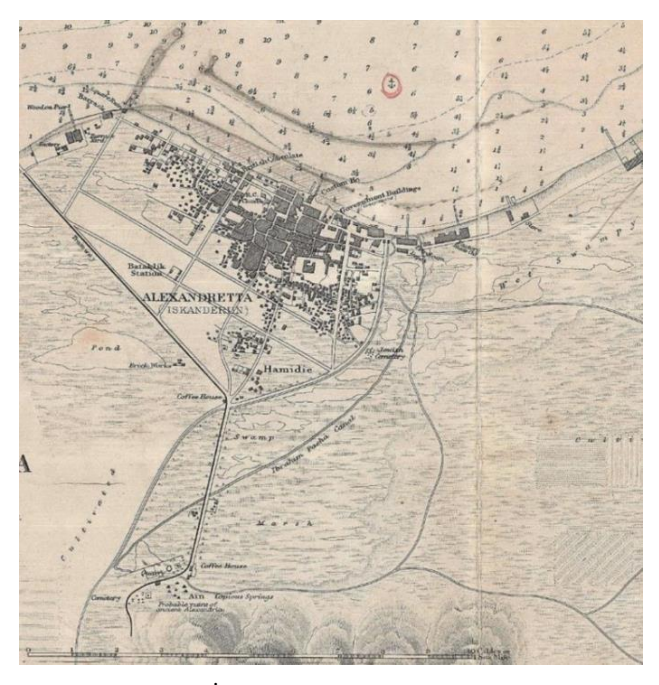


Fig. 1. 1916 map of İskenderun depicting early shoreline, swamps and marshes, and built areas [obtained from the National Library of Turkey by Nalça (2018)].

The Iskenderun shoreline was built out during the city's development. The 1916 shoreline depicted in Fig. 1 approximately aligns with present-day Atatürk Boulevard. It represents the approximate border between reclaimed and naturally formed land. The shoreline was further built out prior to 1969 as indicated by a declassified KH-4 Corona satellite image presented in Taftsoglou et al. (2023). The approximate 1916 and 1969 historic shoreline extents and location of the İbrahim Paşa channel are traced on the post-earthquake observations map in Fig. 2. These provide a basis to delineate potential subsurface constraints on the extent of liquefaction and lateral spreading ground deformations.

## 3 POST-EARTHQUAKE FIELD OBSERVATIONS

### 3.1 Liquefaction and lateral spreading

Post-earthquake observations of perishable

liquefaction effects in İskenderun have been well documented by reconnaissance teams following the earthquakes (e.g., METU 2023, Cetin et al. 2023, Moug et al. 2023). Fig. 2 indicates locations of liquefactioninduced sediment ejecta indicated by the aforementioned field teams soon after the earthquake events. These field observations indicate liquefaction occurred primarily in the reclaimed shoreline areas (e.g., post-1916 fills). Sediment ejecta was most heavily concentrated in the Cay District (near the mouth of the historic İbrahim Paşa channel) and inundated Atatürk Boulevard in this area (Cetin et al. 2023). A total of 22 buildings in İskenderun were surveyed by Moug et al. (2023), with liquefactioninduced settlements ranging from negligible to over 700 mm. Damage to coastal facilities following the earthquakes included the partial collapse of a pilesupported naval base wharf, extensional displacements along pier and jetty structures, and the settlement of armor stones making up the rubble mound seawall along much of the shoreline.

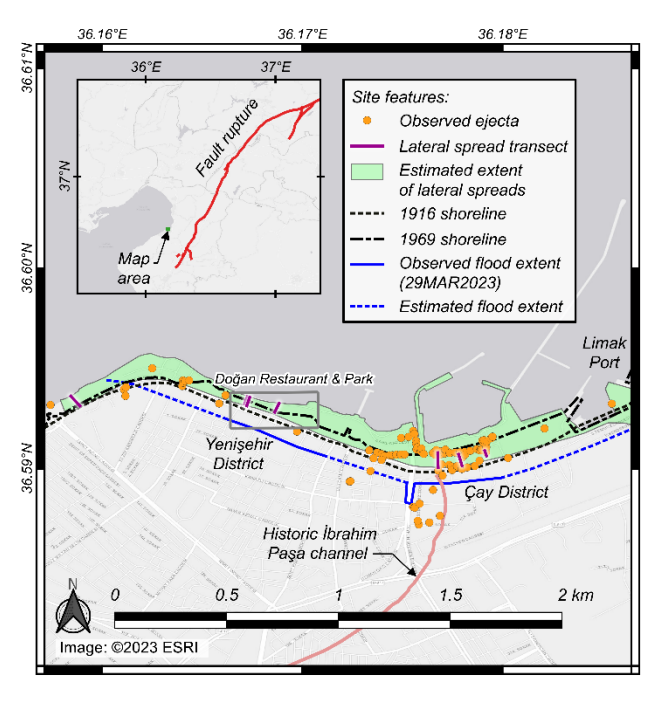


Fig. 2. Map of early shoreline extents and post-earthquake observations in İskenderun (background image: ESRI 2011).

Field observations of extensional ground cracks indicative of lateral spreading extended from the western shoreline of Iskenderun to the Limak Port, as mapped in Fig. 2. Several lateral spreading transects are indicated in Fig. 2 where detailed measurements of accumulated displacements were obtained by Moug et al. (2023). Observations at the Doğan restaurant and Emekliler park area are detailed and discussed herein.

## 3.2 Post-earthquake flooding

Images circulating over the news and social media indicated flooding in İskenderun on February 6, 2003 soon after the  $M_{\rm w}$  7.8 mainshock. Residents of

Iskenderun also reported unusually frequent flooding in the waterfront areas, over the weeks following the earthquakes. These reports from residents were consistent with observations by the GEER team of several building owners pumping water from their basements on March 28.

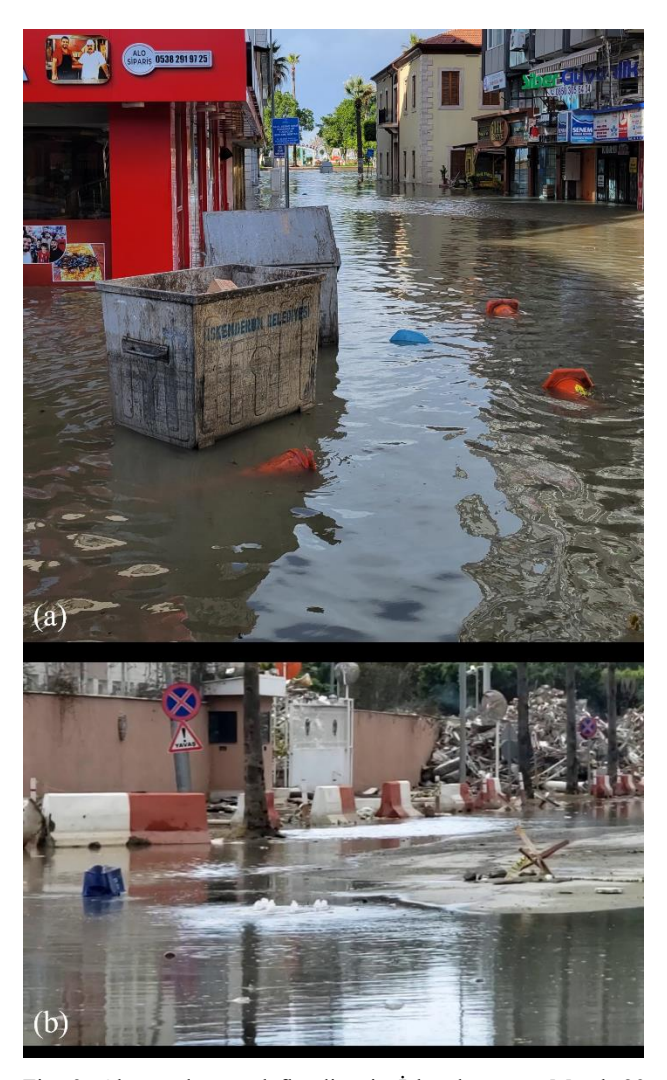


Fig. 3. Observed coastal flooding in İskenderun on March 29, 2023: (a) flood water and debris observed along Mareşal Fevzi Çakmak Street, over 250 m from the shoreline (36.5912N, 36.1698E); and (b) flood water expelling from drain along Bahçeli Sahil Evler Street in the Çay District (36.5900N, 36.1768E).

The GEER team encountered notable flooding on March 29, 2023 (Fig. 3). On this day, moderate rainfall and strong southwesterly Lodos winds impacted the Iskenderun area. The flooding extended from about 150 m to over 250 m inland, as indicated in Fig. 2. Flooding advanced at least two roads in from the shoreline, including past Mareşal Fevzi Çakmak Street (Fig. 3a). Along Bahçeli Sahil Evler Street in the Çay District, water was observed to flow out of a storm drain cap (Fig. 3b), likely due to reports of a damaged water drainage system (METU 2023). The coastal storm surge on March 29 uplifted and displaced rubble mound stones making up the seawall and caused the partial collapse of the

waterfront Teysir restaurant indicated in Fig. 4. When the team returned to İskenderun on April 1, flooding had largely diminished, but standing water remained in some locations.

## 4 CASE HISTORY: DOĞAN RESTAURANT & EMEKLILER PARK

The Doğan restaurant (36.1671N, 36.5934E) and Emekliler park case history site is located along the central shoreline of İskenderun, in the Yenişehir District, as indicated in Fig. 2 and detailed in Fig. 4. The ground surface generally has a gentle slope towards the shoreline of 1-2°. Several extensive ground cracks were observed parallel to the shoreline between the seawall and Atatürk Boulevard (Fig. 5a). A park bench situated along the shorefront walkway appeared stable during a reconnaissance visit on March 28, 2023, but had sunken into the ground following the March 29 storm surge and flood (Fig. 5b). A one-story patio dining structure within the restaurant exhibited several large ground cracks through the floor and exterior walls (Fig. 5c).

On March 28, the armor stones making up the seawall in this area appeared to have settled by up to 0.5 to 1 m relative to pre-earthquake street-view imagery (Google 2022). On April 1, the armor stones were re-arranged about 1 m higher, and the reinforced concrete parapet wall behind the stones was more heavily damaged (Fig. 5a-b). It is unclear whether the existing stones displaced to this configuration during the March 29 storm surge, or additional stones were manually added for temporary coastline protection.

Lateral spreading transects were measured by taking the distance from the inside of the waterfront seawall to all visible cracks along the transect. The widths of the crack openings were also measured and accumulated along each transect using the methodology of Robinson et al. (2010) to obtain seaward displacements. The transects were typically selected in areas where crack openings could be easily identified (e.g., near paved walkways, not obscured by grass or other vegetation).

Transects LS-2 and LS-3 measured on April 1, 2023 indicated maximum lateral ground displacements of 77 cm and 73 cm over distances of 41 m and 45 m, respectively. Both transects extended from the rubble mound seawall to the front (south side) of the Doğan restaurant. LS-2 was taken about 1 m away from the Doğan patio exterior walls, and LS-3 was taken 10 m to the east of LS-2. While both transects are within post-1916 reclaimed land, about half of the transect lengths are located seaward of the approximate post-1969 shoreline. The distribution of accumulated lateral displacements along LS-2 and LS-3 are depicted in Fig. 6a to be fairly consistent with each other. Interestingly, higher displacement rates (i.e., increased shear strain) along LS-2 and LS-3 were measured within 15 m from the seawall, which may coincide with post-1969 reclaimed fill.

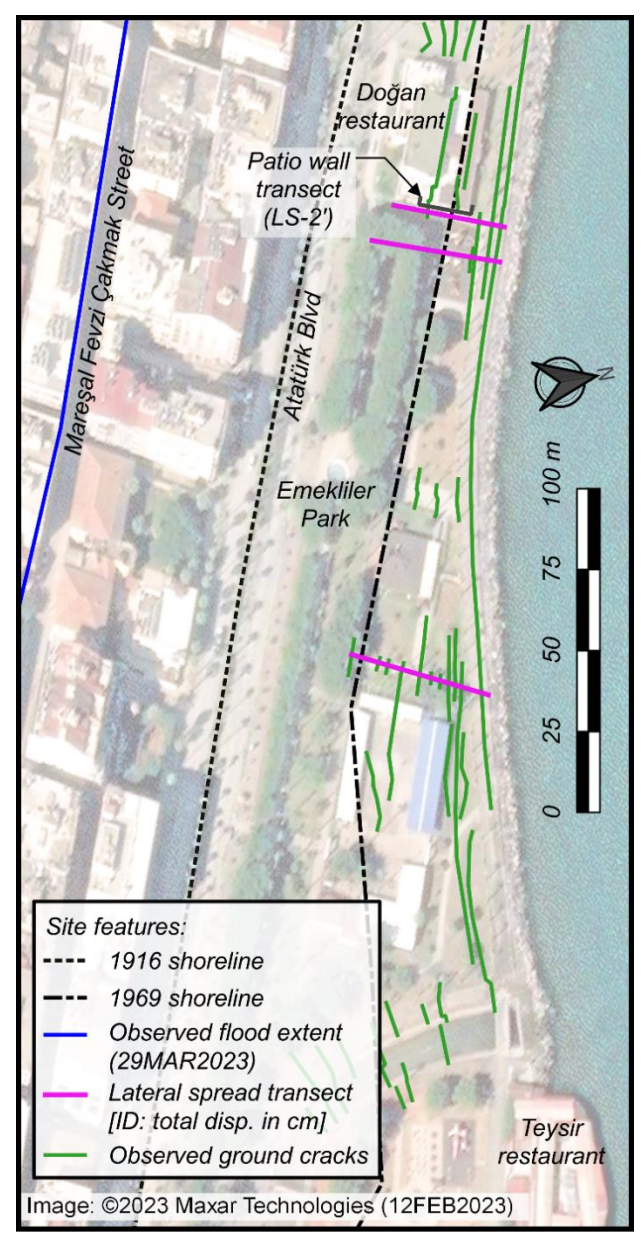


Fig. 4. Map of Doğan restaurant and park lateral spread site. Background image from Maxar (2023) is dated February 12, 2023.

Transect LS-2' only considered cracks along the base of the exterior patio wall and concrete fence of the Doğan restaurant (right side of Fig. 5c). The cracks were measured over a limited distance from the north edge of the patio to the north edge of the two-story restaurant building. This transect was plotted in Fig. 6a to allow a direct comparison with LS-2, by matching the accumulated displacements at the north edge of the patio (i.e., 14.8 m from the seawall). Cracks were concentrated with a total width of 10.5 cm along the column at the south edge of the patio (~25 m from the seawall), and a width of 14 cm at the north edge of the restaurant building (~28.5 m from the seawall). Despite this structurally-induced concentration of cracking along the building at certain locations, the total displacements along the extent of LS-2' approximately matched those along LS-2 and LS-3.



Fig. 5. Lateral spreading damage observed on April 1, 2023: (a) park area along transect LS-4 (36.5930N, 36.1687E); (b) sunken park bench and ground deformation behind Doğan restaurant patio (36.5937N, E36.1672E), and (c) cracking in patio along back of Doğan restaurant building (36.5935N, 36.1671E)

Transect LS-4 was measured on March 28 and April 1, 2023 (before and after the 29 March storm) with respective maximum lateral ground displacements of 140 cm and 147 cm over the same distance of 52 m. The spread extended from the seawall to an area within the Emekliler park beyond which cracks were no longer visible. The entirety of spreading observed along this transect extended seaward of the estimated 1969 shoreline, with the exception of a 10 cm wide crack located 3 m south of the 1969 shoreline. No other cracks were observed south of this transect. Figure 6b depicts a fairly constant rate of accumulated lateral displacements along the length of LS-4. This displacement rate approximately matches LS-2 and LS-3 within 15 m of the seawall (i.e., the portions of those transects seaward of the 1969 shoreline). The inconsistency of the 1969 shoreline relative to the transects may indicate

differences in the subsurface soils that would cause LS-4 to spread nearly twice as much as LS-2 and LS-3. Additionally, there may be differences in the free-face heights at these sites. The measured increase in maximum displacements at LS-4 by 7 cm before and after the storm may have been due to scour and dislocation of surficial features (e.g., concrete pavers) during the storm, additional movements continuing since the earthquake or worsened by storm surge loading, measurement errors, or other effects.

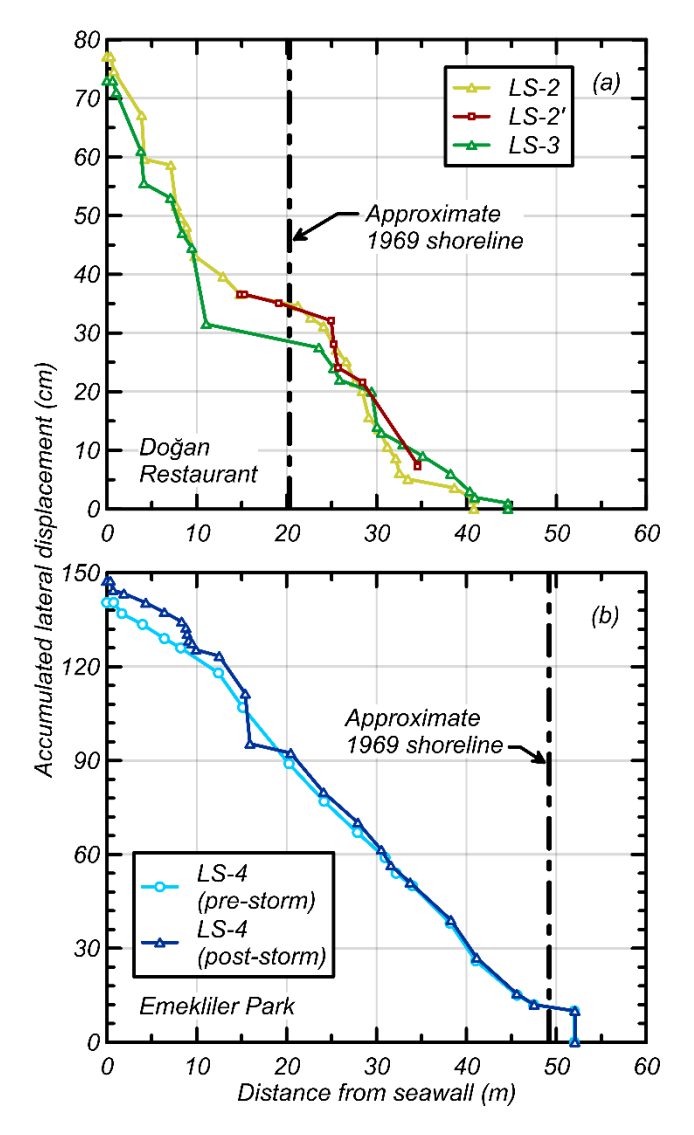


Fig. 6. Accumulated lateral displacements obtained from crack measurements relative to distance from the seawall, for transects located: (a) adjacent to the Doğan restaurant, and (b) within Emekliler park (~150 m east of the Doğan restaurant). Note that symbols indicate individual crack measurements that accumulate from the landward extent of the transect (where no movement is assumed).

## 5 DISCUSSION

The cascading influence of liquefaction-induced ground movements in low-lying coastal areas have been postulated as a key contributor to increased flood hazards and permanent land submergence following several past earthquakes. Dramatic subsidence and loss of land to the sea within coastal areas in the 1964 Great Alaska, 1992 Flores Island Indonesia, and 1999 Kocaeli earthquakes have been associated with subsurface liquefaction and lateral spreading (e.g., Lemke 1967, Ishihara 2003, Cetin et al. 2004). The occurrence of increased post-earthquake flooding hazards in Iskenderun is believed to be similarly associated with widespread liquefaction-induced ground movements.

The lateral spreading ground measurements described herein are not a direct measure of vertical subsidence relative to the sea level that would be expected to directly increase flood risks. Vertical subsidence is typically difficult to measure at case history sites, unless precise pre- and post-event elevation data (e.g., from global positioning systems (GPS) data or similar) is available. However, the magnitude and extent of lateral spreading observed along much of the Iskenderun shoreline suggests a ubiquity of liquefiable sediments that have volumetrically reconsolidated following the dissipation of pore pressures.

Several other factors likely contributed to increased flooding risks in Iskenderun. The loss of freeboard due to settlement of the seawall, has been unable to adequately inhibit coastal storm surge. Nonetheless, settlement and instability of the seawall may have similarly been initiated by the liquefaction and lateral spreading within subsurface soils. Damage to the water drainage system (METU 2023, Cetin et al. 2023) and the consequent build-up of water along pavement and other non-draining surfaces likely slowed the ability for water to recede following each storm. Change detections of Synthetic Aperture Radar (SAR) images also indicate that İskenderun has been continually subsiding over the four years prior to the earthquake at rate of over 40 mm/year (Papageorgiou et al. 2023). This could suggest other large-scale subsidence or tectonic mechanisms.

Work is currently underway to evaluate postearthquake SAR change detections and coastal storm surge models, to help elucidate the mechanisms contributing to the post-earthquake floods. Subsurface investigations are also underway to better understand the ground conditions relative to liquefaction triggering and general ground subsidence.

### 6 CONCLUSIONS

Liquefaction-induced damage and flooding along the İskenderun shoreline were observed following the 2023 Kahramanmaraş earthquakes. An understanding of the development of İskenderun and early shoreline extents help to indicate subsurface constraints affecting the extents of liquefaction and lateral spreading. The lateral spreading case history at the Doğan restaurant illustrates the importance of subsurface constraints for evaluating lateral spreading, and potential influences of coastal storm surge inundation for exacerbating spreading.

Liquefaction and lateral spreading are postulated as likely contributing factors to the observed post-earthquake floods, among other factors. Additional subsurface data and evaluations are needed to further clarify the mechanisms contributing to the post-earthquake floods.

### **ACKNOWLEDGEMENTS**

The work of the GEER Association is supported in part by the National Science Foundation (NSF) through the Engineering for Civil Infrastructure Program under Grant No. CMMI1826118. Any opinions, findings, and conclusions or recommendations expressed in this material are those of the authors and do not necessarily reflect the views of the NSF. Any use of trade, firm, or product names is for descriptive purposes only and does not imply endorsement by the U.S. Government. The GEER Association is made possible by the vision and support of the NSF Geotechnical Engineering Program Directors: Dr. Giovanna Biscontin, Dr. Richard Fragaszy, and the late Dr. Cliff Astill. Researchers from the Middle East Technical University received support from the Turkish government. Additionally, Zemin Etüd vs Tasarim A.Ş. provided financial support for a team member. The authors are grateful for the support of Dr. H. Turan Durgunoğlu (ZETAS), Dr. Murat Bikçe (İskenderun Technical University), Dr. Papageorgiou (National Technical University Athens), Dr. Jorge Macedo (Georgia Tech), Dr. Halil Sezen (The Ohio State University), Dr. Ethan Kubatko (The Ohio State University), Dr. Charles Toth (The Ohio State University), and Mr. Ahmet Palalioglu (a local building owner).

## REFERENCES

- Cetin, K. O., Youd, T. L., Seed, R. B., Bray, J. D., Stewart, J. P., Durgunoglu, H. T., Lettis, W., & Yilmaz, M. T. (2004). "Liquefaction-Induced Lateral Spreading at Izmit Bay During the Kocaeli (Izmit)-Turkey Earthquake." J. of Geotech. and Geoenviron. Engineering, Vol. 130, No. 12. 10.1061/(ASCE)1090-0241(2004)130:12(1300)
- Cetin, K.Ö., Bray, J.D., Frost, J.D., Hortacsu, A., Miranda, E., Moss, R.E.S., Stewart, J.P. (2023). "February 6, 2023 Turkiye Earthquakes: Report on Geoscience and Engineering Impacts." Earthquake Engineering Research Institute, LFE Program, GEER Association Report 082, May 6, 2023. https://10.18118/G6PM34
- Esri (2023). "World Light Gray Base." Accessed September 10, 2023. <a href="https://services.arcgisonline.com/ArcGIS/rest/services/Canvas/World Light Gray Base">https://services.arcgisonline.com/ArcGIS/rest/services/Canvas/World Light Gray Base</a>
- Google (2022). [Google street view imagery of Iskenderun shoreline dated January 2022; uploaded by user Makro 360]. Retrieved September 1, 2023.
- Ishihara, K. (2003). "Characteristics of Waterfront Landslides Induced by Earthquakes." Proc. of Int. Conf. on Fast Slope Movements-Prediction and Prevention for Risk Mitigation, Naples, Italy.
- Lemke, R. W. (1967). "Effects of the Earthquake of March 27, 1964, at Seward, Alaska." U. S. Geological Survey Professional Paper 542-E, 43 p.

- 7) Maxar Technologies (2023). "Imagery Basemap, Catalog ID: 10300100E1B9D900, Quadkey: 031133021303, Satellite: WV02, Collection date: Feb 12, 2023, 12:16:32-08:00." <maxar.com/open-data/turkey-earthquake-2023>
- Middle East Technical University (METU) (2023).
  "Preliminary Reconnaissance Report on February 6, 2023, Pazarcık Mw=7.7 and Elbistan Mw=7.6, Kahramanmaraş-Türkiye Earthquakes." Report No. METU/EERC 2023-01, 20 February.
- Moug, D., Bassal, P., Bray, J. D., Çetin, K. Ö., Kendir, S. B., Şahin, A., Çakır, E., Söylemez, B., & Ocak, S. (2023).
  "February 6, 2023 Türkiye Earthquakes: GEER Phase 3 Team Report on Selected Geotechnical Engineering Effects."
  Geotechnical Extreme Events Reconnaissance (GEER) Association, Report No. GEER-082-S1, 30 June. <a href="https://doi.org/10.18118/G6F379">https://doi.org/10.18118/G6F379</a>
- 10) Nalça, C. (2018). "Transformation of İskenderun Historic Urban Fabric from Mid 19th Century to the end of the French Mandate Period." Masters Thesis, Izmir Institute of Technology, Graduate School of Engineering and Sciences.
- 11) Orukoğlu, N. & İşhani, S. S. (2010). "Hatay Province, İskenderun District, İskenderun Municipality, Microzonation Study Report." Denge Engineering Ltd., Antakya, Turkey.
- 12) Papageorgiou, E., Foumelis, M & Delgado Blasco, J.M. (2023). Pre-seismic Sentinel-1 PSI surface motion measurements for the area affected by the February 2023 Türkiye–Syria earthquakes (1.0) [Data set]. Zenodo. https://doi.org/10.5281/zenodo.7672169
- 13) Reitman, N. G., Briggs, R. W., Barnhart, W. D., Thompson, J. A., DuRoss, C. B., Hatem, A. E., Gold, R. D., Akçiz, S., Koehler, R. D., Mejstrik, J. D., Collett, C. (2023). "Fault rupture mapping of the 6 February 2023 Kahramanmaraş, Türkiye, earthquake sequence from satellite data: U.S. Geological Survey data release, <a href="https://doi.org/10.5066/P98517U2">https://doi.org/10.5066/P98517U2</a>
- 14) Robinson, K., Cubrinovski, M., Kailey, P., Orense, R. (2010). "Field Measurements of Lateral Spreading following the 2010 Darfield Earthquake." Proc., Ninth Pacific Conference on Earthquake Engineering Building an Earthquake-Resilient Society, Auckland, New Zealand.
- 15) Taftsoglou, M., Valkaniotis, S., Papathanassiou, G., Karantanellis, E. (2023). "Satellite Imagery for Rapid Detection of Liquefaction Surface Manifestations: The Case Study of Türkiye-Syria 2023 Earthquakes. Remote Sensing, 15, 4190. https://doi.org/10.3390/rs15174190.
- 16) Ulu, U et al. (2002). "1:500,000 Scale, Geological Map of Turkey: Hatay." General Directorate of Mineral Research and Exploration, Ankara, Turkey.